



Noble metal-modified TiO₂ thin film photocatalyst on porous steel fiber support

Hongfan Guo^{*}, Marianna Kemell, Mikko Heikkilä, Markku Leskelä

Laboratory of Inorganic Chemistry, Department of Chemistry, University of Helsinki, P.O. Box 55, Helsinki FI-00014, Finland

ARTICLE INFO

Article history:

Received 1 September 2009

Received in revised form 14 January 2010

Accepted 18 January 2010

Available online 25 January 2010

Keywords:

Porous steel fiber

Atomic layer deposition

Sputtering

TiO₂

Photocatalysis

ABSTRACT

Through-porous steel fiber matrix with high specific surface area and self-support strength was examined as the support of TiO₂ film photocatalyst. TiO₂ was uniformly and conformally deposited onto the surface of the metal skeleton of the porous steel fiber matrix via atomic layer deposition method so that the porosity as well as gas permeability of the matrix is maintained. For further improving the photocatalytic activity, noble metals (Au and Pt/Pd alloy) were sputtered onto the surface of TiO₂ photocatalyst. The photodegradation of methyl orange was used for evaluating the photocatalytic properties. The results show that compared with TiO₂ films deposited on flat Si wafers, TiO₂ films on the porous support display higher photocatalytic activities, owing to their higher specific surface areas. The photocatalytic activity of TiO₂ on porous support was not enhanced by Au, while it was remarkably improved by Pt/Pd. The TiO₂ photocatalysts were also analyzed by scanning electron microscopy and X-ray photoelectron spectroscopy.

© 2010 Elsevier B.V. All rights reserved.

1. Introduction

TiO₂ is a very promising photocatalyst due to its strong oxidation capacity, high photochemical and biological stability, non-toxicity and low cost. Both powdery and thin film TiO₂ can be used as photocatalyst, but the later is often preferred because there are several problems with the powdery TiO₂ [1–4]: (i) difficulty and high cost in the separation and recovery of the catalyst from suspension; (ii) easy aggregation of the suspended particles; (iii) difficulty in application to continuous flow systems. These problems can be easily solved by immobilizing TiO₂ onto inert support [5]. Moreover, TiO₂ film is very convenient for many special practical applications, such as in hospitals and hotels to kill viruses and bacteria [6–8]. Hence, more efforts are still needed for fixing TiO₂ onto proper supports with suitable immobilization technology.

Several materials have been extensively studied as the effective support of TiO₂, e.g., glass, silica, quartz, clay, ceramics, zeolites. Porous metal fiber material made of metal skeleton and pores/voids [9] (see Fig. 1a and b) is a type of structural and functional material. Due to possessing many properties of both metal and porous material, it can be used in separation, filtration, gas distribution, heat exchangers, electromagnetic-wave shield, etc [10,11]. Therefore, and because of its large specific surface area and high self-support strength, it deserves attention and study as the structural and functional support of TiO₂ film photocatalyst.

There are several optional ordinary methods for immobilizing TiO₂ onto different supports, such as sol–gel method, physical vapor deposition, chemical vapor deposition, liquid phase deposition and doctor blade, however, they all have some limitations [12–15] in preparing conformal and uniform TiO₂ film on above-mentioned porous metal fiber material to maintain the porosity of the support. Atomic layer deposition (ALD) is a special layer-by-layer chemical gas phase deposition technique capable of coating extremely complex shapes with a conformal material layer of high quality [16–20]. Its special self-limiting growth mechanism, i.e., deposited material is produced by the precursors saturatively chemisorbed on support surface as monolayer, ensures that material is deposited using all the support surface as the template and grows by one layer per cycle. Thus, ALD is an ideal method for preparing TiO₂ coating on such kind of porous material. We have developed an ALD reactor configuration [13] for rapid and uniform coating of through-porous materials. In this configuration, the precursors are forced to flow through the substrate to fast disperse to all the surface of the substrate.

In this paper, a process for preparing TiO₂ film photocatalyst is described. In this flow, TiO₂ is first coated on porous steel fiber support using the above-mentioned ALD reactor configuration. Due to the uniform and conformal deposition of TiO₂ only on the surface of the metal skeleton, many properties of porous steel fiber support, such as porosity and gas permeability, are maintained. It is well-known that the photocatalytic activity of TiO₂ originates from the highly reactive electron–hole pairs generated by absorbing incident photons, but these photogenerated electrons and positively charged holes often suffer from fast recombination resulting in decrease of the quantum yield [21–25]. Loading noble

^{*} Corresponding author. Tel.: +358 919150229; fax: +358 919150198.
E-mail address: Hongfan.Guo@helsinki.fi (H. Guo).

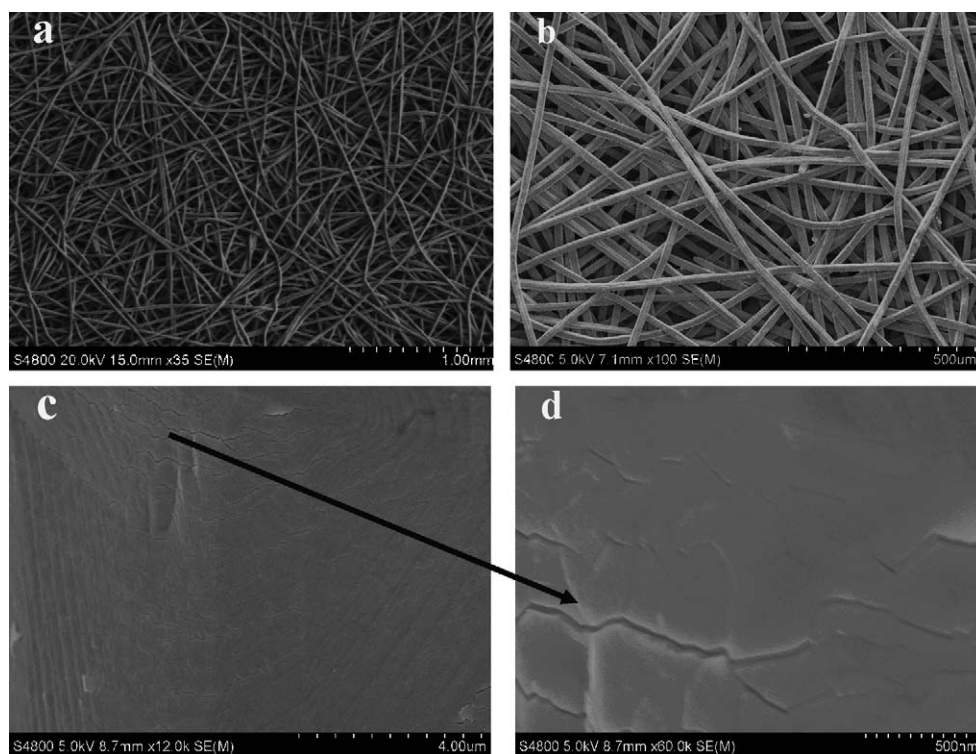


Fig. 1. Top-view SEM images of TiO₂-coated metal fibers with different magnifications.

metal onto the surface of TiO₂ has been proven to have the ability to improve the separation of photogenerated electrons and holes to enhance photocatalytic efficiency [1,4,26–29]. Consequently, in the present paper effort was put to further increase the photocatalytic activity of TiO₂ on porous support by loading with noble metal. The usual methods for loading noble metal onto the surface of TiO₂ are deposition–precipitation and photodeposition [30]. Here we employ sputtering method to directly deposit noble metal onto the photocatalytically effective outside surface of photocatalyst. This method is very clean and easy to be accomplished in a few minutes.

2. Experimental

2.1. Preparation of photocatalysts

The through-porous metal matrix (received from NV Bekaert SA, Belgium) consisted of stainless steel 316L fibers and was about 0.5 mm thick. TiO₂ coating was deposited in a SUNALE ALD reactor (Picosun Oy, Espoo, Finland) using TiCl₄ and water as precursors, and nitrogen as carrier and purging gas. In order to enable faster deposition in this highly porous sample, a special flow through arrangement was used that forces the precursor vapors to flow through the porous sample [13]. The times used for every step in one growth cycle, i.e. (1) exposing TiCl₄, (2) purging reaction chamber, (3) exposing water, and (4) purging reaction chamber again [18,31], were 0.2 s, 6.0 s, 0.2 s and 6.0 s, respectively. The growth cycle was repeated 1000 times at 250 °C. For comparison, TiO₂ films were also prepared on planar Si wafers with the same number of ALD cycles.

Noble metals were deposited on the photocatalyst by sputtering method. The sputtering was performed in a high resolution sputter coater (Cressington 208HR, Cressington Scientific Instruments Ltd, UK). The sputter coater is fitted with a very accurate terminating thickness monitor/controller (MTM-20 high resolution thickness controller) so that different nominal

deposition thickness (NDT) can be chosen. The target materials used were Pt/Pd alloy (80/20 by weight, Cressington), and pure gold (Cressington). NDT is the thickness quantified as a flat metallic film deposited on a flat substrate, so the metal amount can be figured out by the formula: $\text{weight} = \text{volume}_{\text{metal}} \times \text{density}_{\text{metal}} = (\text{area}_{\text{substrate}} \times \text{NDT}) \times \text{density}_{\text{metal}}$. The densities of Au and Pt/Pd are 19.3 g cm⁻³ and 19.52 g cm⁻³, respectively. So 1 nm in the NDT of Au and Pt/Pd represents 19.3×10^{-7} g Au and 19.52×10^{-7} g Pt/Pd per cm² photocatalyst, respectively. The validity of this calculation was verified by sputtering Au films on flat Si substrates and determining their thicknesses by EDX. The thicknesses were calculated from EDX data with a GMRFILM program [32] using the bulk density of Au. The calculation was found to be valid at least for NDT > 5 nm. It is possible that the accuracy is less for thinner NDTs, but this could not be evaluated because the relative error of EDX measurement increases with decreasing film thickness, thus reducing the accuracy of thickness determination. For comparison, noble metals were also sputtered onto Al₂O₃ films prepared on Si wafers via ALD method (trimethylaluminum and water as precursors) and used for studying photocatalytic properties of metal nanoparticles on an inert support.

2.2. Characterization of photocatalysts

Scanning electron microscopy (SEM) images and EDX spectra were obtained by a Hitachi S-4800 field emission scanning electron microscope with Oxford INCA 350 energy dispersive X-ray microanalysis system. The XRD patterns were measured with a PANalytical XPert PRO MPD diffractometer with CuK α radiation. The X-ray photoelectron spectroscopy (XPS) measurements were performed with a PHI Quantera SXMTM scanning X-ray MicroprobeTM spectrometer. The binding energy was corrected using C1s core line as reference. The specific surface area was measured using N₂ adsorption–desorption via an Autosorb-1-C surface area and pore size analyzer (Quantachrome, UK).

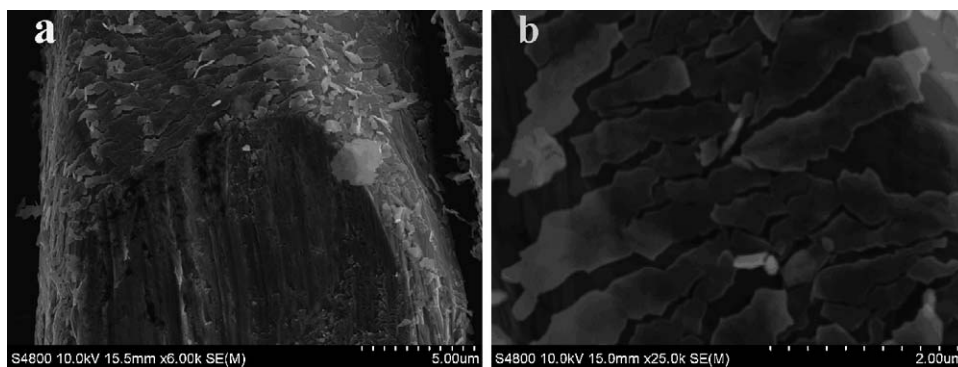


Fig. 2. SEM images of a TiO₂ film taken near the cut edge of the metal fiber.

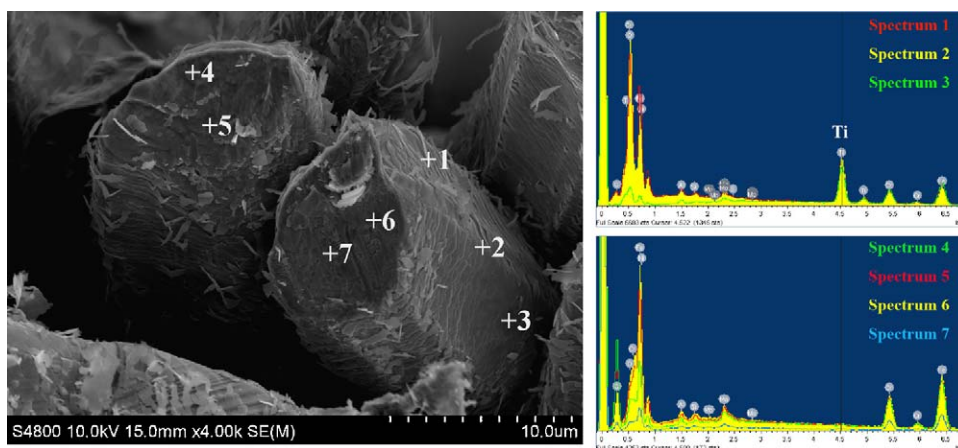


Fig. 3. Cross-sectional SEM image of TiO₂-coated metal fibers, and EDX spectra measured from the locations denoted with numbers in the SEM image.

2.3. Photocatalytic activity measurement

Photocatalytic activity was evaluated by the photocatalytic decomposition of methyl orange (MO) aqueous solution (2×10^{-5} M) at ambient temperature. MO, a typical azo-dye used in textile industry, is very stable and is commonly used as the probe for evaluating photocatalysts [1,2,4,33]. An 18 W Blacklight-Blue UV lamp (Sylvania, Japan, with the peak maximum at 365 nm) was used as the irradiation source. Light irradiation intensity at photocatalyst was about 26 W/m². Different thin film photocatalysts (nominal areas 2 cm²) were first immersed into 3 mL MO solution in UV transparent disposable cuvette, and kept in the dark for 1 h to attain the adsorption-desorption equilibrium of MO and dissolved oxygen on the surface of TiO₂ [34,35]. After that, the irradiation was started. The concentration of MO in the solution as a function of irradiation time was measured by the absorbance of the MO at its absorption maximum ($\lambda_{\text{max}} = 465$ nm) using a UV-vis spectrophotometer (HP Hewlett-Packard 8453).

3. Result and discussion

Fig. 1 shows the typical top-view SEM images with different magnifications of TiO₂ films on the metal fiber. The low-magnification images (Fig. 1a and b) indicate that the diameter of the fiber is about 25 μm , while the length is far more than 1 mm. The high-magnification image (Fig. 1c) displays that TiO₂ is uniformly coated on the surface of the fiber. The cracks (resulting from the slight bend of fiber when cutting samples) exhibited in Fig. 1d verify the existence of TiO₂ coating on the fiber. But this proof is not sufficient, so cross-sections of the fibers were studied. The part near the cross-section can deform during cutting and thus

the TiO₂ coating there will be torn up. A lot of TiO₂ fragments near the cross-section can be seen (Fig. 2), which can also prove the existence of TiO₂ coating. The associated EDX spectra (Fig. 3) further show that TiO₂ has been coated on the fiber. The Ti can be found on the surface of the fiber (sites 1–3), while there is no Ti in the cross-section (sites 4–7). In the XPS survey spectrum (Fig. 4), there are only extremely strong Ti and O peaks and neglectable weak peaks of Fe, indicating that almost all the surface of steel fiber is coated by TiO₂. There are no big differences between the low-magnification images of coated fiber (such as Fig. 1a and b) and uncoated fiber (not shown). Owing to the uniform and conformal coating of TiO₂ on the whole surface of steel fiber, the porosity as

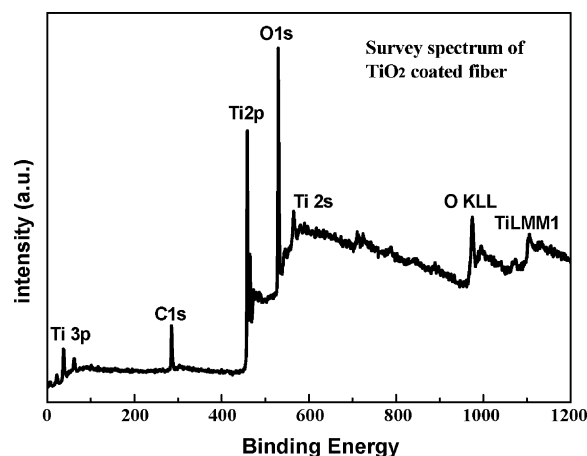


Fig. 4. XPS survey spectrum of TiO₂-coated steel fiber.

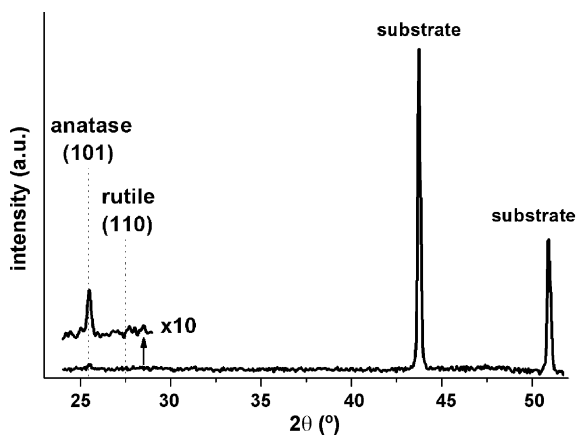


Fig. 5. X-ray diffractogram of a TiO₂-coated metal fiber sample.

well as gas permeability of porous steel fiber is maintained. It is very difficult to achieve similar coating quality by other methods, such as sol–gel.

In the XRD patterns of a TiO₂-coated metal fiber sample (Fig. 5), the two sharp reflections originate from the porous steel matrix. Because the characteristic peaks of the matrix are extremely strong, those of TiO₂ present as very weak ones. From the ten times multiplied data, a reflection at low angles attributed to anatase phase [36] can be seen clearly. TiO₂ is deposited as anatase which is generally considered as the best crystalline form for TiO₂ photocatalyst [37]. Noble metals could not be detected by XRD, probably due to their low amounts.

SEM images confirm that noble metals are evenly dispersed over the whole outer surface of the TiO₂-coated metal fiber matrix. For Au (Fig. 6A), it is obvious that particle size increases with the increase of NDT. Gold exists as nanoparticles at low NDT and as nano-islands at higher NDT. It is very difficult to detect Au by SEM when using NDT of 0.5 nm, indicating that the particle size is in that case extremely small. For Pt/Pd, on the other hand, no nanoparticles or nano-islands can be found. This indicates that Pt/Pd is dispersed much better than Au.

TiO₂ can photocatalytically mineralize harmful organic contaminants when it is irradiated with light energy greater than its band gap (3.2 eV). MO is commonly used as the probe for evaluating photocatalysts, and its degradation mechanism has been clarified elsewhere [38]. MO can be mineralized into CO₂, H₂O, NO₃[−], NH₄⁺ and SO₄^{2−} by photogenerated reactive species,

such as photogenerated electrons, •OH and •O₂ free radicals. Fig. 7 illustrates the photocatalytic decomposition of MO under UV light in the presence of different TiO₂ thin film photocatalysts. Compared with TiO₂ on flat Si, TiO₂ on porous support shows an improvement in photodecomposition rate of MO owing to its higher specific surface area (41.88 m²/g). Although Au has been proven to be capable of enhancing the photocatalysis for TiO₂ [39], including in the decomposition of MO [1,40], it seems here to play a role as an impurity and decreases the photocatalytic activity. In our case, the photocatalytic activity of TiO₂ on porous support is decreased even by loading only a small amount of Au, while it can be doubled by depositing Pt/Pd alloy. The degradation rate is clearly enhanced when using Pt/Pd NDT of only 0.4 nm. Further increasing Pt/Pd amount does not improve the photocatalysis markedly, so the optimum NDT is at about 0.4 nm. Photocatalytic activity begins to decrease at the NDT of 2 nm, but it is still better than for a bare TiO₂ film. From Fig. 7c it can be seen that MO cannot be decomposed by the Pt/Pd sputtered onto the Al₂O₃, so Pt/Pd itself is photocatalytically inert and the improvement in photocatalysis results from the synergetic effect of high surface area TiO₂ and Pt/Pd. Interestingly, in contrast to the case of TiO₂ on porous support, the photocatalytic activity of TiO₂ on flat support could not be improved remarkably within wide span of NDT (Fig. 7c). In order to estimate the effect of MO absorption on the high surface area photocatalyst samples, a dark test was performed where the samples including noble metal-modified samples were kept in dark in the MO solution for 2 h without illumination. None of the samples showed any detectable changes in the MO concentration during adsorption. Therefore, the role of adsorption on the MO concentration decreases during photocatalysis test can be considered negligible and the decrease of the MO concentration under the UV light irradiation is attributed to the photocatalytic degradation.

XPS measurements were carried out to investigate the chemical states of the deposited noble metals, Ti and O. Fig. 8 shows the Ti2p and O1s XPS spectra of different samples. For unmodified TiO₂ on porous support, the binding energies of Ti2p peaks were 458.7 eV and 464.6 eV, attributed to Ti⁴⁺2p_{3/2} and Ti⁴⁺2p_{1/2}, respectively [41–43]. The O1s XPS spectra are asymmetric, which shows besides lattice oxygen at least one adsorbed oxygen species also exist near the surface [43–45]. Both Ti2p peaks and the O1s peaks obviously shift to higher binding energies after depositing noble metal. In Jiang et al.'s study on isocyanate-modified TiO₂ [46], they also found these distinct shifts toward higher binding energy because of chemical interaction (not adsorption) between TiO₂ and isocyanate molecules. From this point, it can be predicted that

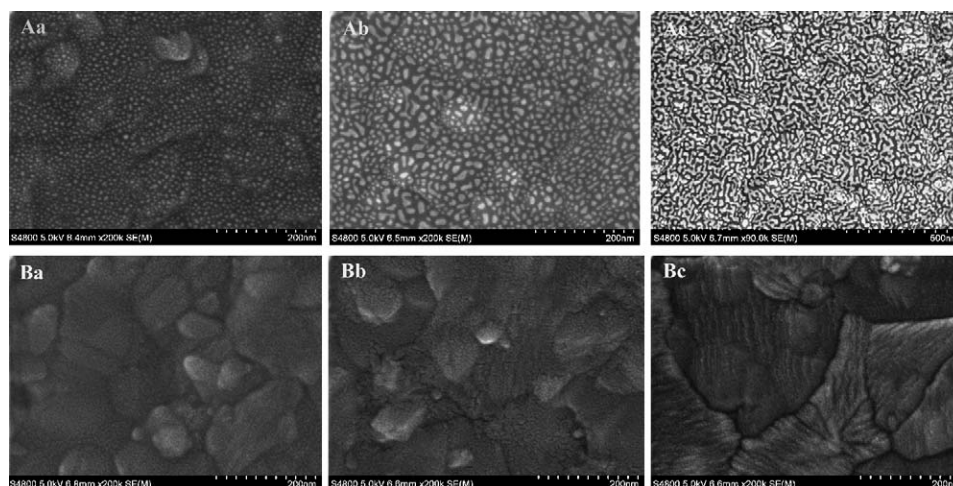


Fig. 6. SEM images of noble metal-modified TiO₂ on porous support with nominal deposition thicknesses (NDT) of (a) 1.0 nm; (b) 2.0 nm; (c) 3.0 nm (A: Au-modified; B: Pt/Pd-modified).

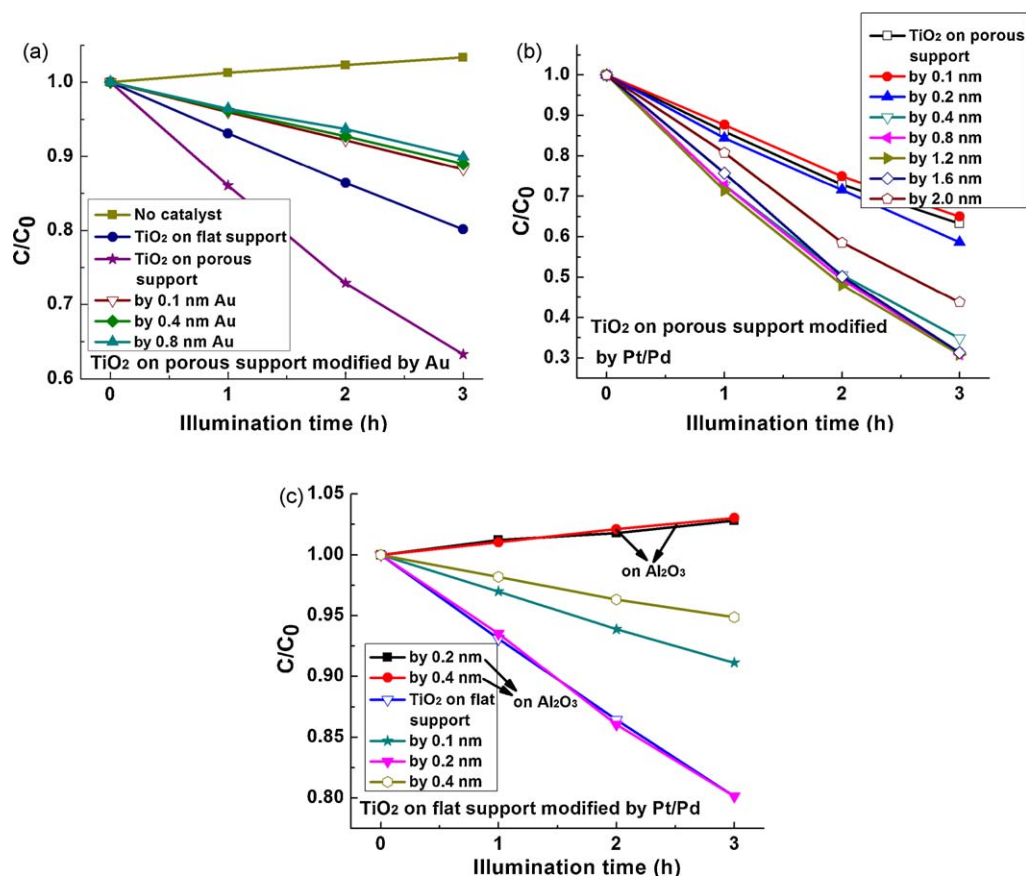


Fig. 7. Photocatalytic degradation of MO under UV irradiation in the presence of different photocatalysts (C_0 : initial MO concentration; C : MO concentration at given degradation time).

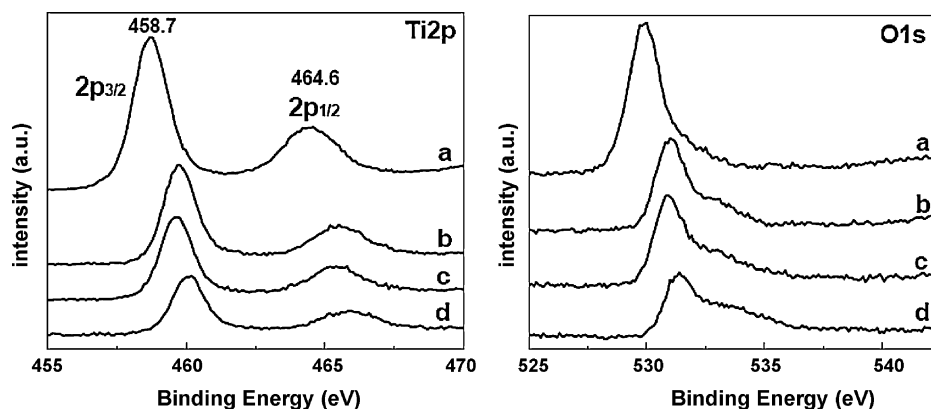


Fig. 8. XPS spectra of Ti₂p and O 1s: (a) unmodified, (b) 0.4 nm Au-modified, (c) 0.4 nm Pt/Pd-modified and (d) 0.8 nm Pt/Pd-modified TiO₂ on porous support.

noble metals have a chemical interaction with TiO₂ to some extent and do not simply physically contact with the TiO₂ surface. This interaction may be caused by the large kinetic energy of sputtered atoms which bombard and deposit on the TiO₂ surface.

The XPS spectra of noble metal are shown in Fig. 9. It can be seen that the binding energies of Au_{4f_{7/2}} and Au_{4f_{5/2}} are 83.8 eV and 87.4 eV, respectively. According to the previous reports [47,48], Au is deposited mostly as Au⁰. The comparison between the binding energies of doublet peak of Pt_{4f} reported by Kim et al. [49,50] and the present study suggests that the majority of Pt exists as PtO_{ads} (Pt with adsorbed oxygen). This form of Pt as well as PtO can be seen markedly in the highly dispersed Pt [50]. Standard binding

energies of Pd²⁺3d_{5/2} and Pd⁰3d_{5/2} are about 336.4 eV and 335.3 eV, respectively [44,51]. XPS spectra in Fig. 9 show that the peak of Pd_{3d_{5/2}} shifted by +0.5 eV to 335.8 eV, indicating that Pd is partly oxidized.

Atomic ratio of O to Ti in unmodified, 0.4 nm Au-modified, 0.4 nm Pt/Pd-modified and 0.8 nm Pt/Pd-modified TiO₂ on porous support measured by XPS is 2.891/1, 2.801/1, 4.023/1 and 4.350/1, respectively. The O to Ti ratio decreases a little after depositing Au, while it increases distinctly after depositing Pt/Pd. The increased O to Ti ratio means the enhancement in the content of surface adsorbed oxygen species [44]. Although the content of surface oxygen species did not increase after depositing Au, the amount of

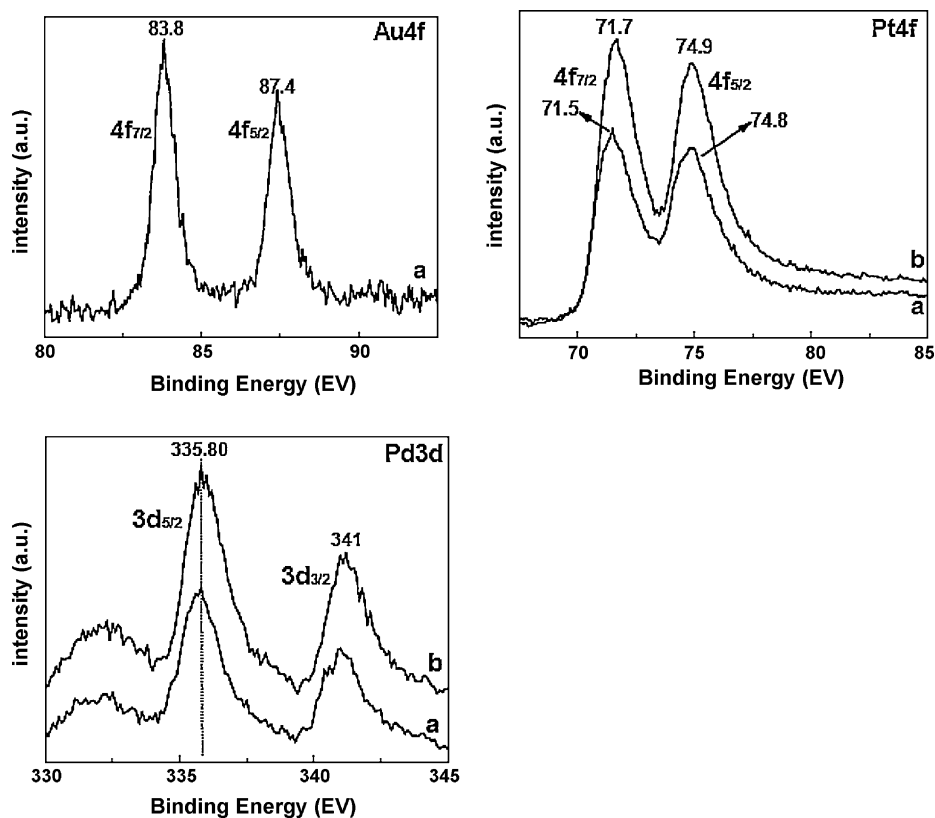


Fig. 9. XPS spectra of loaded noble metal in (a) 0.4 nm and (b) 0.8 nm noble metal-modified TiO₂ on porous support.

various surface oxygen species have changed because the O1s peaks are apparently different from that of unmodified TiO₂ on porous support. In photocatalytic reactions, adsorbed oxygen plays an important role [44,45,52]. Chemisorbed oxygen, such as –OH, can easily capture photoinduced holes, while physisorbed oxygen, such as O₂, can capture photoinduced electrons. Sequentially, they will produce strong oxidants, such as $\cdot\text{OH}$ and $\cdot\text{O}_2$ free radical, to oxidize organic substances. The increase in surface oxygen by Pt/Pd is thus helpful for improvement of photocatalysis.

However, the change in the amount of surface oxygen species caused by noble metal cannot fully explain the change of photocatalytic activity with the increase in the NDT of noble metal shown in Fig. 7. According to previous reports [34,53], Fermi energy of metal particles increases with decreasing particle size due to quantum size effect. When metal particles are too large, electrons cannot be transferred to adsorbed O₂ because the energy level of adsorbed O₂ is higher than that of bulk metal; contrarily, when metal particles are too small, electrons cannot be transferred from TiO₂ to metal particles because the Fermi energy of metal particles is higher than that of TiO₂ conduction band [34]. Therefore, metal particles must be with appropriate size under which the energy level of metal is between those of TiO₂ conduction band and adsorbed O₂ so that photogenerated electrons can be transfer to metal and then be captured by adsorbed O₂, resulting in the valid separation of photogenerated electrons and holes. In the present paper, the impact of particle size should be large because metal is dispersed evenly on the whole photocatalytically effective TiO₂ surface. It can be seen from the SEM images that the particle size of Au increases very fast with the increase in the NDT, so a suitable particle size of Au is hard to get by sputtering method. While for the sputtered Pt/Pd, a proper size can be reached when using the NDT of 0.4 nm. Further increase of NDT does not impact photocatalysis very much because the particle size of Pt/Pd increases very slowly. Only when using the NDT of 2.0 nm,

the particle size begins to get too large. It seems that the particle size of Pt/Pd on the flat TiO₂ increases faster with the increase in the NDT due to the low surface area and so the proper size is also hard to get.

Proper amount of noble metal loaded on the surface of TiO₂ is operative in prohibiting photogenerated electrons and the holes from recombining to increase the photocatalytic efficiency; while excessive noble metal will become electron/hole recombination center, and also produce the inability of the holes to reach the interface, so that photocatalytic efficiency is decreased instead [1,54–58]. For Au its surface concentration has been proven to be crucial for photocatalytic property. Subramanian et al. [59] showed that different Au species, Au⁰ and Au (III), only at low surface concentrations are beneficial. The optimum molar ratio of total Au to TiO₂ colloid is around 0.03/1.5 for both Au species. At high surface concentration, Au will act as electron/hole recombination center. In the present paper the Au amount seems to be too high in all cases. For instance, atomic ratio of Au to Ti in 0.4 nm Au-modified case is 7.43/24.36 as measured by XPS. Therefore, maybe the high surface concentration of Au is another reason for the decreasing photocatalytic activity.

4. Conclusions

In summary, porous steel fiber material can be used as an effective support of TiO₂ thin film photocatalyst. ALD method is an excellent method for preparing uniform TiO₂ coating on this kind of porous support allowing to maintain the porosity of the support. Sputtering is a suitable method for the modification of such film photocatalyst with Pt/Pd to enhance photocatalytic activity. The whole preparation process of noble metal-modified TiO₂ on porous support is well controlled. Sputtered Au and Pt/Pd behaved differently: Au formed rather large nanoparticles while Pt/Pd dispersed better with very small particle size. Small amounts of Pt/

Pd on high surface area TiO₂ enhanced the photocatalysis, while Au showed only negative effects. The maintenance of porosity as well as gas permeability, together with other excellent properties of steel fiber, makes noble metal-modified TiO₂-coated metal fibers a promising candidate for structural photocatalyst.

Acknowledgements

The authors gratefully acknowledge the financial support from the Academy of Finland (Project Nos. 123248, 124189), and the help in the photocatalytic activity measurement provided by Viljami Pore. Eveliina Repo (University of Kuopio) is also thanked for the surface area measurement.

References

- [1] I.M. Arabatzis, T. Stergiopoulos, D. Andreeva, S. Kitova, S.G. Neophytides, P. Falaras, *J. Catal.* 220 (2003) 127–135.
- [2] L. Andronic, A. Duta, *Thin Solid Films* 515 (2007) 6294–6297.
- [3] S. Jung, S. Kim, N. Imaishi, Y. Cho, *Appl. Catal. B* 55 (2005) 253–257.
- [4] M. Huang, C. Xu, Z. Wu, Y. Huang, J. Lin, J. Wu, *Dyes Pigments* 77 (2008) 327–334.
- [5] M.V. Phanikrishna Sharma, V. Durga Kumari, M. Subrahmanyam, *Chemosphere* 73 (2008) 1562–1569.
- [6] S. Gelover, P. Mondragón, A. Jiménez, *J. Photochem. Photobiol. A* 165 (2004) 241–246.
- [7] L. Armelao, D. Barreca, G. Bottaro, A. Gasparotto, C. Maccato, C. Maragno, E. Tondello, U.L. Štangar, M. Bergant, D. Mahne, *Nanotechnology* 18 (2007) 7, 375709.
- [8] C. Wu, L. Tzeng, Y. Kuo, C.H. Shu, *Appl. Catal. A* 226 (2002) 199–211.
- [9] P.S. Liu, K.M. Liang, *J. Mater. Sci.* 36 (2001) 5059–5072.
- [10] J. Banhart, *Prog. Mater. Sci.* 46 (2001) 559–632.
- [11] B. Zhang, T. Chen, *Appl. Acoust.* 70 (2009) 337–346.
- [12] J. Yang, Y. Han, J. Choy, *Thin Solid Films* 495 (2006) 266–271.
- [13] M. Kemell, M. Ritala, M. Leskelä, R. Groenen, S. Lindfors, *Chem. Vap. Depos.* 14 (2008) 347–352.
- [14] H. Kim, S. Lee, Y. Han, J. Park, *J. Mater. Sci.* 40 (2005) 5295–5298.
- [15] A. Mills, A. Lepre, N. Elliott, S. Bhopal, I.P. Parkin, S.A. O'Neill, *J. Photochem. Photobiol. A* 160 (2003) 213–224.
- [16] R.L. Puurunen, *J. Appl. Phys.* 97 (2005) 121301–121352.
- [17] M. Ritala, M. Leskelä, *Nanotechnology* 10 (1999) 19–24.
- [18] M. Leskelä, M. Ritala, *Angew. Chem. Int. Ed.* 42 (2003) 5548–5554.
- [19] M. Ritala, K. Kukli, A. Rahtu, P.I. Räisänen, M. Leskelä, T. Sajavaara, J. Keinonen, *Science* 288 (2000) 319–321.
- [20] M. Ritala, M. Kemell, M. Lautala, A. Niskanen, M. Leskelä, S. Lindfors, *Chem. Vap. Depos.* 12 (2006) 655–658.
- [21] U.I. Gaya, A.H. Abdullah, *J. Photochem. Photobiol. C* 9 (2008) 1–12.
- [22] H. Einaga, M. Harada, S. Futamura, T. Ibusuki, *J. Phys. Chem. B* 107 (2003) 9290–9297.
- [23] V. Iliev, D. Tomova, R. Todorovska, D. Oliver, L. Petrov, D. Todorovsky, M. Uzunova-Bujnova, *Appl. Catal. A* 313 (2006) 115–121.
- [24] F.B. Li, X.Z. Li, *Appl. Catal. A* 228 (2002) 15–27.
- [25] J. Kim, J. Lee, W. Choi, *Chem. Commun.* 6 (2008) 756–758.
- [26] J. Zou, C. Chen, C. Liu, Y. Zhang, Y. Han, L. Cui, *Mater. Lett.* 59 (2005) 3437–3440.
- [27] C. Cai, J. Zhang, F. Pan, W. Zhang, H. Zhu, T. Wang, *Catal. Lett.* 123 (2008) 51–55.
- [28] H. Chen, S. Chen, X. Quan, H. Yu, H. Zhao, Y. Zhang, *J. Phys. Chem. C* 112 (2008) 9285–9290.
- [29] B. Tian, C. Li, F. Gu, H. Jiang, *Catal. Commun.* 10 (2009) 925–929.
- [30] V. Iliev, D. Tomova, L. Bilyarska, G. Tyuliev, *J. Mol. Catal. A* 263 (2007) 32–38.
- [31] M. Ritala, M. Leskelä, E. Nykänen, P. Soininen, L. Niinistö, *Thin Solid Films* 225 (1993) 288–295.
- [32] R.A. Waldo, *Microbeam Anal.*, San Francisco Press, 1988, pp. 310–314.
- [33] Y. Chen, S. Liu, H. Yu, H. Yin, Q. Li, *Chemosphere* 72 (2008) 532–536.
- [34] B. Tian, J. Zhang, T. Tong, F. Chen, *Appl. Catal. B* 79 (2008) 394–401.
- [35] X. Lin, F. Huang, W. Wang, Z. Shan, J. Shi, *Dyes Pigments* 78 (2008) 39–47.
- [36] International Centre for Diffraction Data (ICDD), Card 21–1272.
- [37] C. Guillard, J. Disdier, J. Herrmann, C. Lehaut, T. Chopin, S. Malato, J. Blanco, *Catal. Today* 54 (1999) 217–228.
- [38] I.K. Konstantinou, T.A. Albanis, *Appl. Catal. B* 49 (2004) 1–14.
- [39] C. Yogi, K. Kojima, N. Wada, H. Tokumoto, T. Takai, T. Mizoguchi, H. Tamiaki, *Thin Solid Films* 516 (2008) 5881–5884.
- [40] A. Orlov, D.A. Jefferson, M. Tikhov, R.M. Lambert, *Catal. Commun.* 8 (2007) 821–824.
- [41] X. Zhang, Q. Liu, *Appl. Surf. Sci.* 254 (2008) 4780–4785.
- [42] J. Zhu, F. Chen, J. Zhang, H. Chen, M. Anpo, *J. Photochem. Photobiol. A* 180 (2006) 196–204.
- [43] J.F. Marco, A. Cuesta, M. Gracia, J.R. Gancedo, P. Panjan, *Thin Solid Films* 492 (2005) 158–165.
- [44] L. Jing, D. Wang, B. Wang, S. Li, B. Xin, H. Fu, J. Sun, *J. Mol. Catal. A* 244 (2006) 193–200.
- [45] L. Jing, Z. Xu, X. Sun, J. Shang, W. Cai, *Appl. Surf. Sci.* 180 (2001) 308–314.
- [46] D. Jiang, Y. Xu, D. Wu, Y. Sun, *Appl. Catal. B* 88 (2009) 165–172.
- [47] K.Y. Ho, K.L. Yeung, *J. Catal.* 242 (2006) 131–214.
- [48] Y. Liu, L. Juang, *Langmuir* 20 (2004) 6951–6955.
- [49] K.S. Kim, N. Winograd, R.E. Davis, *J. Am. Chem. Soc.* 93 (1971) 6296–6297.
- [50] B. Ohtani, K. Iwai, S. Nishimoto, S. Sato, *J. Phys. Chem. B* 101 (1997) 3349–3359.
- [51] V. Iliev, D. Tomova, L. Bilyarska, L. Petrov, *Catal. Commun.* 5 (2004) 759–763.
- [52] M.I. Litter, *Appl. Catal. B* 23 (1999) 89–114.
- [53] S. Altunata, K.L. Cunningham, M. Canagaratna, R. Thom, R.W. Field, *J. Phys. Chem. A* 106 (2002) 1122–1130.
- [54] P.V. Kamat, M. Flumiani, A. Dawson, *Colloids Surf. A* 202 (2002) 269–279.
- [55] S. Sakthivel, M.V. Shankar, M. Palanichamy, B. Arabinthoo, D.W. Bahnemann, V. Murugesan, *Water Res.* 38 (2004) 3001–3008.
- [56] H. Tada, F. Suzuki, S. Yoneda, S. Ito, H. Kobayashi, *Phys. Chem. Chem. Phys.* 3 (2001) 1376–1382.
- [57] Z. Shan, J. Wu, F. Xu, F. Huang, H. Ding, *J. Phys. Chem. C* 112 (2008) 15423–15428.
- [58] X. You, F. Chen, J. Zhang, M. Anpo, *Catal. Lett.* 102 (2005) 247–250.
- [59] V. Subramanian, E.E. Wolf, P.V. Kamat, *Langmuir* 19 (2003) 469–474.